Heliyon 9 (2023) e18805

Contents lists available at ScienceDirect

Heliyon

journal homepage: www.cell.com/heliyon

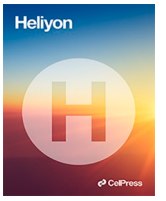

Statistical approach on the inter-yarn friction behavior of the dual-phase STF/ρ-Aramid impregnated fabrics via factorial design and 3D-RSM

Thiago F. Santos [a], Caroliny M. Santos [a], Sanjay Mavinkere Rangappa [b,*], Suchart Siengchin [b], J.H.O. Nascimento [a]

[a] *Postgraduate Program in Chemical Engineering, Technology Center, Federal University of Rio Grande do Norte, Av. Prof. Sen. Salgado Filho, 3000, Natal, Rio Grande do Norte, 59072-970, Brazil*

[b] *Natural Composites Research Group Lab, Department of Materials and Production Engineering, The Sirindhorn International Thai-German Graduate School of Engineering (TGGS), King Mongkut's University of Technology North Bangkok (KMUTNB), Bangkok, Thailand*

A R T I C L E I N F O

Keywords:
Kevlar
Energy absorption
CNT
Carbon nanotube
Pull-out test

A B S T R A C T

Shear thickening fluids (STFs) refer to non-Newtonian fluids of the dilatant variety, wherein their viscosity experiences a significant surge with an escalation in the shear rate. In this investigative work, the friction behavior between yarns (pull-out) and absorption of static and kinetic energy during the phenomenon of friction between yarns in STFs are performed by monophase (MP-STF) adding nano SiO_2 and dual-phase (MP-STF) adding carbon nanotubes. The ρ-Aramid fabrics were reinforced via the "foulard process", and carried out on MP-STF, and DP-STF/ρ-Aramid-impregnated fabrics to evaluate and compare with the enhancement in interfacial friction properties between yarns. The results showed that DP-STF has more significant than MP-STF and MP-STF in ultimate load, kinetic shear stress, static shear stress, and friction energy level effects. The DP-STF exhibits various friction enhancement mechanisms at the yarn interface, leading to higher absorption of static and kinetic energy related to interfacial friction, as indicated by the results obtained. Furthermore, the DP-STF/ρ-Aramid impregnated fabrics exhibited ultimate load (22.23 ± 0.522 N), kinetic shear stress (35.73 ± 0.850 MPa*100), static shear stress (36.28 ± 0.900 MPa*100), and friction energy level (610.33 ± 0.250). Increased ultimate load (581.7% and 180.7%), kinetic shear stress (621.4% and 174.6%), static shear stress (550.5% and 159.1%), and friction energy level (680.2 and 186.7%) compared to WT-STF and MP-STF, respectively. The current discoveries hold immense potential for various applications in the fields of engineering and smart material technologies. These applications span a multiplicity of industries, including sports products, medical advancements, space technology, as well as protective and shielding products.

1. Introduction

The frictional behavior between yarns of woven fabrics is a relevant factor in determining their mechanical properties, particularly in applications, where sliding between yarns is expected [1]. In composite materials, such as those used in protective clothing and

* Corresponding author.
E-mail address: mavinkere.r.s@op.kmutnb.ac.th (S.M. Rangappa).

https://doi.org/10.1016/j.heliyon.2023.e18805
Received 19 April 2023; Received in revised form 27 July 2023; Accepted 28 July 2023
Available online 29 July 2023

ballistic armor, the friction behavior between yarns can greatly influence the energy absorption and deformation resistance of the material [2]. Therefore, understanding and optimizing the friction behavior between yarns on composite fabrics is critical to improve their performance. The test of yarn pullout is a widely used method to measure the interfacial properties in composite for protection materials [3]. The yarn pullout test comprises extracting an individual yarn from the fabric, and analyzing the curve of force-displacement acquired to estimate the properties of interfacial friction [4]. Dual-phase shear thickening fluids are currently being studied due to impact resistance applications due to their unique properties and superior performance over traditional STF [5,6]. The behavior of these colloidal suspensions is mainly determined by the interfacial properties between the different phases. Therefore, understanding the interfacial behavior of dual-phase STF/ρ-Aramid impregnated fabrics is essential for optimizing their performance [7]. The properties of interfacial friction in dual-phase STF/ρ-Aramid impregnated fabrics containing STFs, and ρ-Aramid woven [5]. In 2019, researchers conducted an investigative study on a modified model aimed at fully capturing the rheological characteristics of multi-phase STFs (Suspensions, Slurries, or Soft Matter Fluids). The enhancements made to the flow prediction model for multi-phase STFs resulted in significant improvements, particularly in accurately describing the behavior of shear thinning in these materials [8]. n 2020, other researchers delved into exploring the smart fluids of multi-phase rheology using an innovative intelligent model, marking a groundbreaking milestone in the field. Their pioneering work demonstrated that intelligent modeling proves to be highly efficient, mainly attributed to the algorithm of parameter-free and capability of remarkable fitting. These findings signify a significant advancement in the understanding and application of multi-phase STFs [9].

In recent years, dual-phase composite fabrics composed of STFs and ρ-Aramid fibers have been developed and shown promising results in improving the impact properties of fabric-based composites [10]. STFs are suspensions of colloidal particles that exhibit a unique shear-thickening behavior, which enhances the energy dissipation and, impact resistance of fabric-based composites [11,12]. While ρ-Aramid fabrics are well known for their high strength and stiffness. The combination of STF and ρ-Aramid fabrics has been shown to provide superior energy absorption and impact resistance properties in fabrics used for various applications mainly for personal protection [13].

Several methods be used to understand the friction behaviors between yarns experimental [4,14,15], numerical [16], Modelling [17], and, factorial [18,19]. The factorial design is a statistical method that allows the systematic variation of multiple factors simultaneously, while 3D-RSM is a modeling technique that can visualize the effects of multiple factors on a response variable. By using these techniques, identify the most significant factors that affect the friction between yarns of the fabric-based composite and their levels of frictional resistance. This study, was investigate the friction behavior between yarns of dual-phase STF/ρ-Aramid fabrics using a statistical approach. Was employ a factorial design and 3D-RSM (3-Dimensional Response Surface Methodology) to analyze the impacts of various factors, such as STF type (WT-STF, MP-STF, and DP-STF), and the speed of pull-out (100, 550, and 1000 mm/min), on the inter-yarn friction behavior. The findings obtained from this research endeavor offer significant insights into the interfacial characteristics of dual-phase STF/ρ-Aramid fabrics. This valuable information has the potential to advance the development of fabric-based composites applied to impact and various cut resistance situations such as various applications, including protective clothing, ballistic armor, and other engineering uses, ensuring high-performance outcomes.

2. Materials and methods

High-performance ρ-Aramid fabrics are materials that have been repeatedly used and applied and applied to shear thickening fluids. For all experiments, ρ-Aramid fabrics were used, as exhibited in Table 1.

2.1. Factorial design

Table 2 presents the variables and conditions utilized for the experimental planning in this statistical study, conducted using the statistical software Design Expert 13 [20,21]. The investigation aimed to examine the friction properties behaviour of dual-phase STF/ρ-Aramid impregnated fabrics [19,22] and employed a factorial design of 2^2 with 4 replicates and 1 central point. The response properties (refer to Table 2) were assessed and analyzed through analysis of variance (ANOVA), which involved determining the F-value, the probability of significance (ρ-value), the determination coefficient R^2, and the response surface 3D (RSM) [23].

2.2. Shear thickening fluid preparation

The shear thickening fluids monophase and dual-phase were prepared with polyethylene glycol 400 g/mol as dispersant phase,

Table 1
Material characteristics and Geometric parameters of ρ-Aramid fabrics.

Material characteristics	Geometric parameters
Structure	1x1Taffeta
Grammage	472-522± g/m2
Linear density - Weft	336–344.4 Tex
Linear density - Warp	341–346.1 Tex ±2.56
Weft/cm	7
Warp/cm	7

Table 2
Variables, experimental conditions, and power responses for the study.

Variable	Type	Low		Middle	High	
A - Composition	Numeric	1 (WT-STF)		2 (MP-STF)	3 (DP-STF)	
B – Pull-Out speed	Numeric	100		550	1000	
Design of the power responses for the study						
	Units	Delta (Signal)	Sigma (Noise)	Signal/Noise	Power of A	Power of B
Yarn pull-out force	N	2	1	2	96%	96%
Kinetic shear stress	(MPa)* 100	2	1	2	96%	96%
Static shear stress	(MPa)* 100	2	1	2	96%	96%
Friction energy	mJ	2	1	2	96%	96

ethanol (99%) was used to dilute the STFs, as well as silica (SiO_2 - powder) spherical nanoparticles (20 nm from EVONICK), and carbon nanotubes (CNTs – acquired from university) was utilized as the dispersed phase. For preparation of the MP-STF composition, SiO_2 nanoparticles were added based on the mass percent concentration [24] as exhibited in Table 3; Later on, they were combined and vigorously stirred for over 12 h via sonication to obtain a stable colloidal suspension. To obtain DP-STF, the same procedure used for MP-STF was performed. After the 12 h being mixed and stirred, the 2nd dispersed phase (CNTs) were added to the STF monophase and mixed, stirred for more than 12 h via sonication. So, the preparation of DP-STF was finalized as exhibited in Fig. 1.

2.3. Impregnation in the ρ-Aramid fabrics

The MP-STF and DP-STF were prepared using a process via impregnation called foularding. Initially, was diluted each STFs with ethyl alcohol in 1 ethanol/4 STF, and the ρ-Aramid fabrics were cut into square pieces with dimensions of 11 cm × 11 cm. Each ρ-Aramid fabric was immersed in the STF with different dispersed phases (MP-STF and DP-STF), for 15 min. Then, the ρ-Aramid fabrics were squeezed through a foularding process (0.5 bar pressure and 3 m/min rollers velocity) with the aim of extracting excess Shear thickening fluids. Afterward, the ethanol was eliminated through evaporation using a laboratory stenter machine (75 °C per 1 min and 30 s) [5]. Finally, was produced STF's different dispersed phases.

3. Characterization

3.1. Analysis of scanning electron microscopy (SEM)

After impregnation with MP-STF and DP-STF, the ρ-Aramid fabrics were subjected to a drying process and subsequently characterized using HITACHI scanning electron microscopy (SEM), model TM3000 (Hitachi, Tokyo, Japan). The objective of this analysis was to assess the distinctions among the ρ-Aramid fabrics, namely: untreated ρ-Aramid fabric (WT-STF), ρ-Aramid fabric impregnated with dispersed monophase STF (MP-STF), and ρ-Aramid fabric impregnated with dispersed dual-phase STF (DP-STF).

3.2. Rheological test of STF

The rheological properties of DP-STF – 0.5%, DP-STF – 0.4%, DP-STF – 0.3%, DP-STF – 0.2%, MP-STF, and PEG 400 were tested by rheometer of TA Company. The flat rotor had a diameter of 25 mm, with a spacing value of 0.5 mm. The environment temperatures were 25 °C ± 2 °C. Fig. 2 depicts the viscosity versus shear rate relationship by plotting curves across a shear rate scanning range of 0.1–1000 1/s.

When the mass fraction of Carbon Nanotubes (CNT) reaches 0.5% in the DP-STF, both the initial and peak viscosity of the STF increase simultaneously. This is attributed to the gradual increase of the number of 'new particle groups,' causing a reduction in the distance between the particles, thus impeding their flow. The DP-STF containing 0.5% CNT exhibits significant properties of shear thinning and shear thickening, resulting in a substantially higher peak viscosity compared to DP-STF with 0.4% CNT, 0.3% CNT, and 0.2% CNT, respectively. So, for that reason, it was used DP-STF (with 0.5% CNT) in this statistical approach study.

3.3. Yarn pull-out test

Experiments were conducted utilizing a tensile testing machine (Tensolab 3000 from Mesdan), and samples with dimensions of 10

Table 3
Composition of each shear thickening fluid.

Sample	PEG 400 (%)	SiO_2 (%)	CNTs (%)
WT-STF (without STF)	–	–	–
MP-STF (monophase)	65	35 [5]	–
DP-STF (dual-phase)	65	34.50	0.50

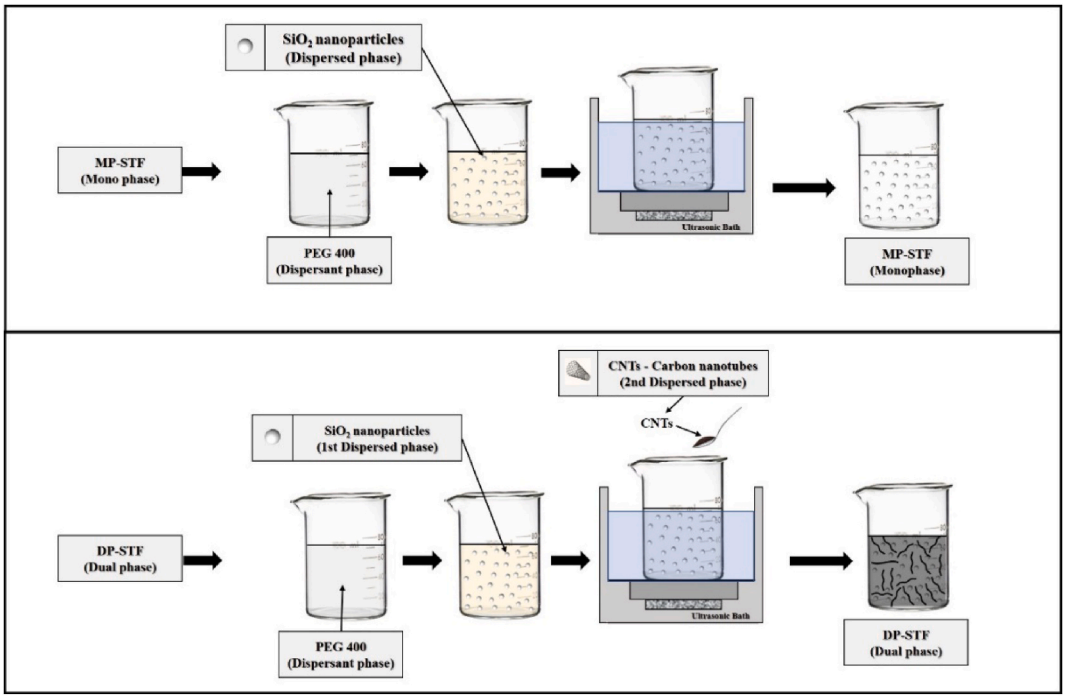

Fig. 1. Illustration of the production process of the different STFs.

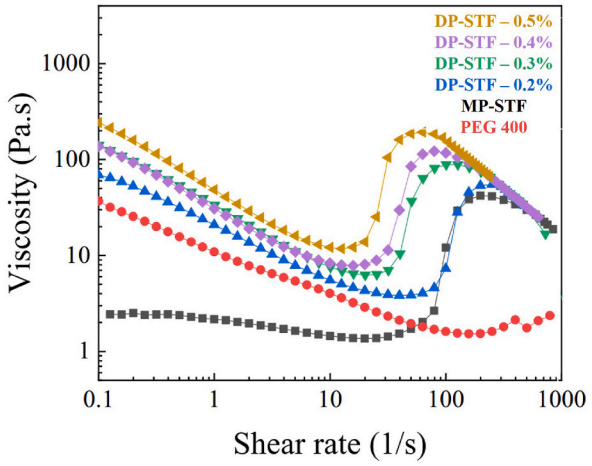

Fig. 2. Rheological performance of PEG 400, MP-STF, and the optimization of DP-STF with CNTs.

cm length and 2 cm width are exhibited in Fig. 3A. This test was used to explore the influence, and behavior of the WT-STF, MP-STF, and DP-STF in the friction among the yarns. A deliberate cut was required below the lower end of the single yarn to ensure its freedom. The tensile test machine's movable jaw was set to three different speeds: 100 mm/min, 550 mm/min, and 1000 mm/min as shown in Fig. 3A, B. To measure the friction force against the yarns, the ρ-Aramid fabric was securely fastened to the bottom jaw of the machine, and a single yarn was then extracted by the movable jaw of the tensile machine, as shown in Fig. 3B.

4. Results and discussions

4.1. Analysis of scanning electron microscopy – SEM

4.1.1. SEM micrographs of shear thickening fluids with MP-STF (M0 and M1) and DP-STF (M2 and M3)

In the case of MP-STF, SEM micrographs typically show regular-shaped SiO_2 particles dispersed throughout the fabric surface.

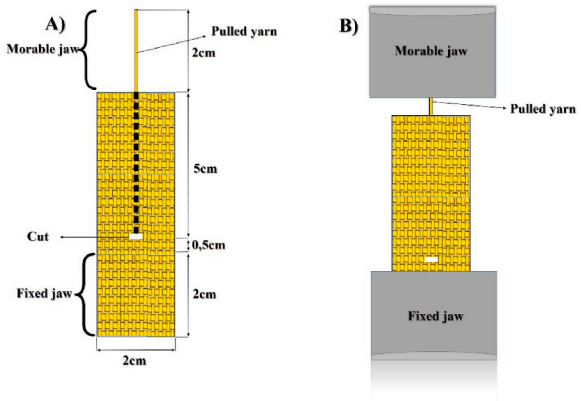

Fig. 3. Representation of (A) test configuration and (B) test on equipment.

These particles are seen to form clusters or agglomerates, which contribute to the shear thickening behavior of the fluid. As exhibited in Fig. 4 (M2, and M3) the SEM micrographs of (DP-STF) typically show a more uniform dispersion of both SiO_2 particles and CNTs throughout the fabric surface [25]. The CNTs act as a "skeleton" to support the SiO_2 particles, preventing their clustering and leading to a more stable and uniform microstructure. This results in enhanced STFs behavior and improved resistance to the force of yarn pull-out, the energy consumed by the interface, static and kinetic friction interface, and protective capabilities. Furthermore, SEM micrographs of DP-STF often reveal a network of interlocking CNTs. SEM micrographs of MP-STF (SiO_2) and DP-STF (SiO_2+CNT) reveal important differences in microstructure that impact the fluid's shear thickening behavior [26].

4.2. Statistical analyzes

Silica (SiO_2) nanoparticles are commonly used as the primary filler in STFs (MP-STF), as they promote improvement its performance compared to WT-STF. However, the addition of a secondary filler (CNTs) to STFs (DP-STF) enhanced the properties as exhibited in Fig. 5. This happens because CNTs form a strong network within the fluid, increasing its strength and viscosity [27]. Additionally, the high proportion of CNTs allows them to form entangled networks, which provide reinforcement and prevent the formation of large clusters of nanoparticles that could lead to sedimentation and separation of the fluid over time [28]. The results showed that DP-STF (SiO_2+CNTs) exhibit higher yarn pull-out forces compared to those MP-STF (SiO_2) and WT-STF (without STF). This is due to the high aspect ratio of CNTs, and they form entangled networks within the STF, which can provide reinforcement and increase the adhesion between the STF and the fibers or yarns [29]. In contrast, MP-STF does not exhibit the same level of reinforcement, and adhesion caused by the absence of entangled networks formed by the nanoparticles [30]. As obtained result, the force of yarn pull-out in MP-STF was inferior to those using DP-STF [31]. In summary, the addition of CNTs to STFs (DP-STF) improves the reinforcement and adhesion

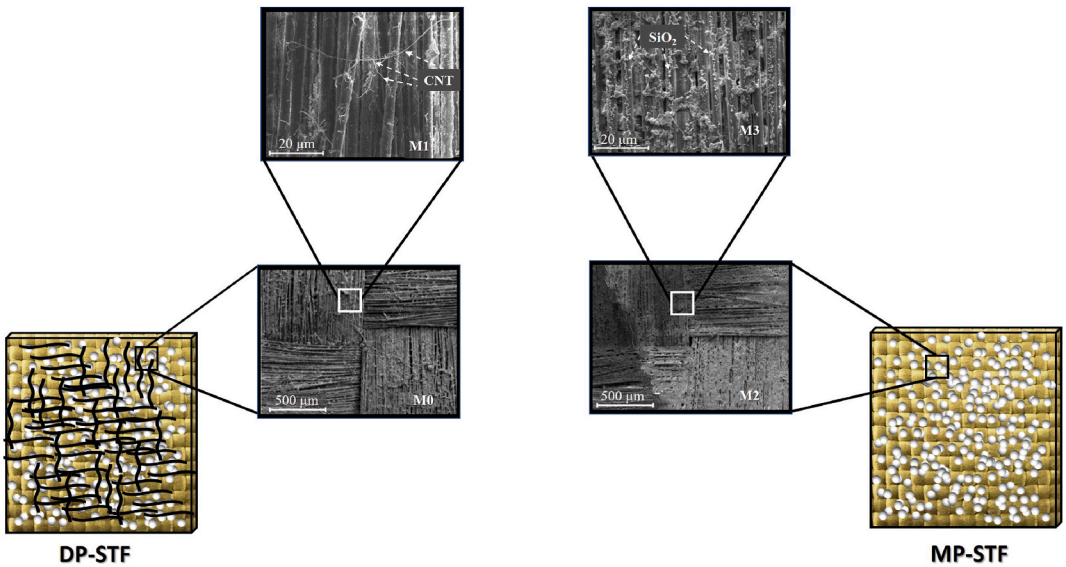

Fig. 4. SEM images of surfaces in (M0 and M1) MP-STF/ρ-Aramid fabrics; (M2 and M3) DP-STF/ρ-Aramid fabrics.

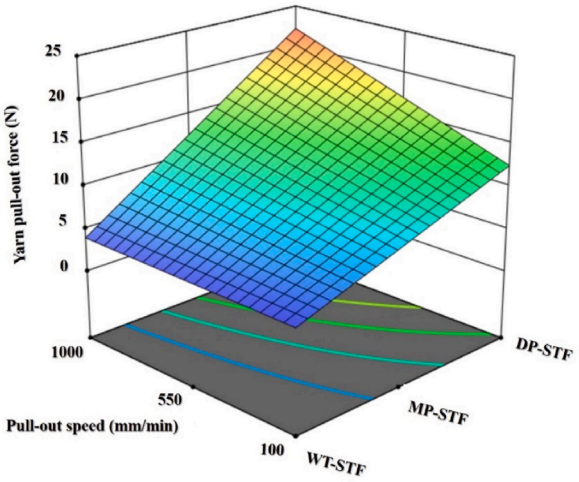

Fig. 5. Result of yarn pull-out force in different shear thickening fluids (WT-STF, MP-STF, and, DP-STF) using 3D surface.

properties of the STF, leading to higher yarn pull-out forces and better overall performance in composite materials for use in personal protection [32]. The speed of the pull-out positively affects the yarn pull-out force in shear thickening fluids (STFs) because it affects the shear rate and fluid viscosity surrounding the fiber or yarn during the test [33]. As the rheological properties in the DP-STF (SiO_2+CNTs) were superior to those of MP-STF (SiO_2) and WT-STF (without STF). When the pull-out was carried out at a higher speed (1000 mm/min), the shear rate of the DP-STF increases more than those of others (MP-STF and WT-STF), which cause a nonlinear increase in its viscosity. This increase in viscosity lead to a higher force of yarn pull-out as STFs becomes more resistant to deformation and flow. On the other hand, when the pull-out test is performed at a lower speed (100 mm/min), the shear rate of the MP-STF and WT-STF decreases drastically compared to DP-STF (SiO_2+CNTs), which causes an intense reduction in its viscosity to MP-STF and WT-STF, this did not happen to DP-STF. Which promotes the protective performance of composite fabrics against impact loads. Then, the high aspect ratio of CNTs allows them to form entangled networks, which prevent the formation of large clusters and separation of the fluid over time. Therefore, the speed of the pull-out test has a significant impact on the force of yarn pull-out in STFs as showed in Fig. 5.

During the test of yarn pull-out in STFs, the energy absorbed by the interface between the fiber or yarn and the STF is a critical parameter that affects the overall performance of the protective fabrics. The level of interface friction energy consumption was affected by the STF type (DP-STF, MP-STF, and WT-STF) and the speed of pull-out used in the test. MP-STF does not exhibit the same level of resistance to fiber or yarn sliding due to the lack of entangled networks formed by the nanoparticles. As a result, the interface friction energy consumption level during yarn pull-out in MP-STF was lower than DP-STF (SiO_2+CNTs). Fig. 6 shows that STFs using a combination of silica nanoparticles and carbon nanotubes (DP-STF) exhibit higher interface friction energy consumption levels during

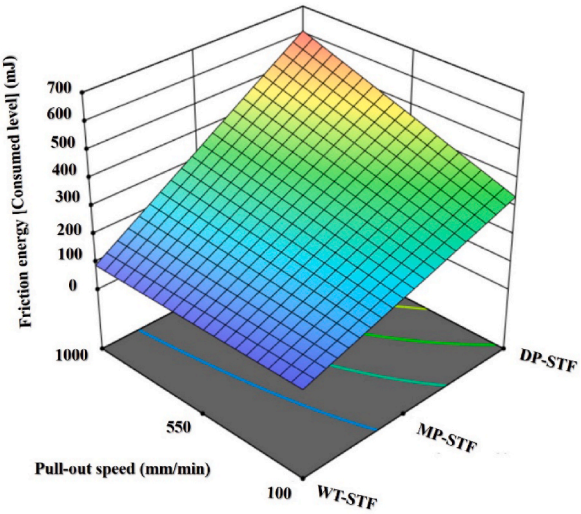

Fig. 6. Result of Friction energy in different shear thickening fluids (WT-STF, MP-STF, and, DP-STF) of using 3D surface.

yarn pull-out tests compared to those MP-STF, and WT-STF [34]. This occurred because the CNTs form entangled networks within the STF, which provide more resistance to the deformation and sliding of the fiber or yarn during the pull-out test. The SiO_2+CNTs (DP-STF) improve the resistance to fiber or yarn sliding and increase the interface friction energy absorption level during the test of pull-out. This lead to better overall performance in protective materials that use shear thickening fluids as a reinforcement. When a yarn is pulled out of an STF, the frictional force between the yarn and the fluid generates energy that is dissipated. The level of energy consumption during yarn pull-out in STFs is influenced by several factors, including the speed of the yarn pull-out. At low speeds of yarn pull-out (100 mm/min), the STF has enough time to flow around the yarn and effectively lubricate its movement, resulting in lower levels of frictional force and energy consumption (MP-STF, and WT-STF) as exhibited in Fig. 6. However, as the speed of pull-out increases (1000 mm/min), the STF is unable to flow around the yarn as quickly, leading to a higher level of frictional force and energy consumption (DP-STF). Therefore, the speed of yarn pull-out is an important factor to consider when designing systems that use STFs for energy absorption or damping purposes, as it can significantly affect the energy dissipation capabilities of the fabrics impregnated.

Static interfacial friction in MP-STF (SiO_2) was inferior to those in DP-STF (SiO_2+CNTs) due to the synergistic effect because CNTs interact with SiO_2 particles to form a more stable and stronger network structure. This enhances the interparticle interactions and increases the rheological properties and STFs behavior in the fluid, resulting in higher interfacial friction. Then, a higher surface area than the CNTs, which allows for more effective contact with the opposing surface, resulting in increased friction significantly higher in DP-STF compared to MP-STF. The increased surface area also provides more sites for the formation of hydrogen bonds and other intermolecular interactions, further enhancing the interfacial friction as exhibited in Fig. 7. CNTs can align themselves in the applied shear direction, creating a more ordered structure that enhances the STFs behavior in the fluid, clearly remarked in behavior of DP-STF. This alignment also increases interfacial friction by creating more contact points between the fluid and the opposing surface [35]. Overall, the DP-STF significantly improve their interfacial friction, making them more effective in protective applications. The static friction interface in shear thickening fluids was affected by yarn pull-out speed (100 mm/min, 550 mm/min, and 1000 mm/min). Pull-out of yarn refers to the process of pulling a yarn or fiber out of a fabric structure. If the yarn is pulled out too slowly (100 mm/min), the STF may have more time to form a stable network around the yarn, resulting in a lower static friction interface. On the other hand, when the yarn is pulled out too quickly (1000 mm/min), the STF may not have enough time to form a stable network around the yarn, resulting in a higher static friction interface. In both DP-STF (SiO_2+CNTs) and MP-STF (SiO_2) the speed at which the yarn was pulled out affected positively the static friction interface compared to WT-STF [21]. However, DP-STF was more affected than the others (MP-STF, and WT-STF), due to the time-dependent behavior of STFs and the formation and breakage of particle networks within the STF as showed in Fig. 7.

The kinetic friction interface in shear thickening fluids (STFs) also was affected by the yarn pull-out speed. Observed that yarn was pulled out of a STF at different speeds as shown in Fig. 8, it can affect the kinetic friction interface between the yarn and the STF (DP-STF, MP-STF, and, WT-STF). Specifically, a slower yarn pull-out speed (100 mm/min) was lead to a lower kinetic friction interface, while a faster yarn pull-out speed (1000 mm/min) leads to a higher kinetic friction interface this phenomenon was observed by DP-STF (SiO_2+CNTs), and MP-STF (SiO_2) except WT-STF. This effect be explained by the time-dependent behavior of STFs. DP-STF (SiO_2+CNTs) exhibit time-dependent behavior superior to MP-STF (SiO_2), where their viscosity and other properties can change over time [36]. This time-dependent behavior is often attributed to the formation and breakage of particle networks within the STF. Then, when a yarn is pulled out of a DP-STF at a higher speed, the STF particles (SiO_2+CNTs) have more time to form a stable network around the yarn. This network can create more points of contact and increase the kinetic friction interface, resulting in higher resistance to motion between the yarn and the STF compared to those prepared only with SiO_2. Finally, the yarn pull-out speed affected

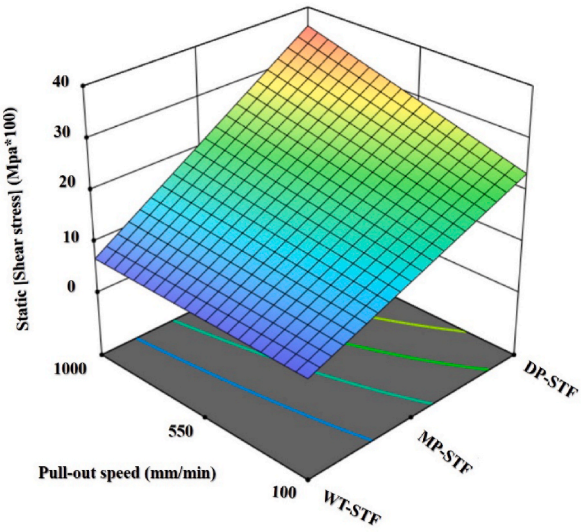

Fig. 7. Result of Static (Shear stress) in different shear thickening fluids (WT-STF, MP-STF, and, DP-STF) of using a 3D surface.

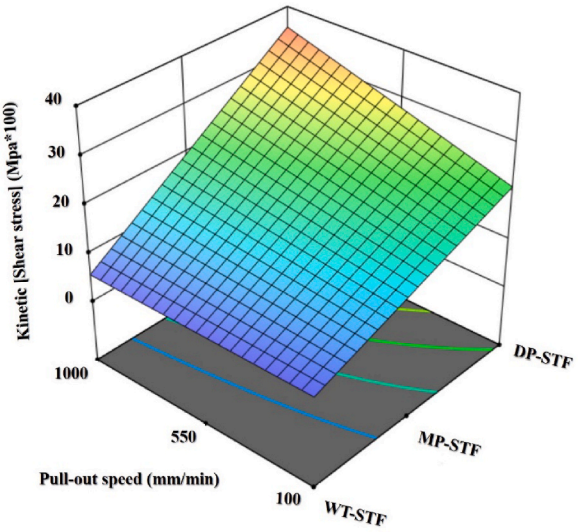

Fig. 8. Result of Kinetic (Shear stress) in different shear thickening fluids (WT-STF, MP-STF and, DP-STF) of using a 3D surface.

both the static and kinetic friction interfaces in DP-STF and MP-STF due to the formation and breakage of particle networks.

The force-displacement curves for fabrics impregnated with different types of STFs - WT-STF, MP-STF, and DP-STF - exhibited distinct characteristics. In Fig. 9b, it can be observed that the friction force during extraction experienced a sudden increase for each variant of STF. This phenomenon is attributed to the presence of a dispersed second phase in DP-STF, which contributes to an additional friction force. Specifically, the DP-STF (SiO2+CNT) demonstrated the highest peak extraction force at 22.3 N, surpassing the WT-STF value of 7.57 N by 194.6%. Furthermore, the introduction of carbon nanotubes (CNT) in the dual-phase STF (DP-STF) enhanced the friction between yarns. This effect impeded the pulled yarn from slipping and hindered the projectile penetration. As a result, the significant factor was the friction between the yarns, which played a critical role in enhancing the dissipation and absorption of kinetic energy during projectile impacts. Additionally, Fig. 9a and b illustrate that the curve of force-displacement in WT-STF at a speed of 1000 mm/min exhibited lowest frictional force of 7.57 N, accompanied by a relatively smaller displacement of 3.3 mm. In summary, the curves of the force-displacement on the fabrics impregnated with different STF variants demonstrated varying friction forces, with the DP-STF (SiO2+CNT) exhibiting the highest extraction force. The incorporation of Carbon Nanotubes (CNT) in the DP-STF resulted in enhanced inter-yarn friction, significantly reducing yarn slippage and greatly improving the fabric's ability to dissipate and absorb kinetic energy from projectile impacts.

In Table 4 shear thickening fluids MP-STF (SiO_2) are generally inferior to those DP-STF (SiO_2+CNTs) for several reasons as an aggregation because SiO_2 particles tend to aggregate in STFs, which results in poor dispersion and reduces their effectiveness in improving the viscosity of the fluid [37]. DP-STF (SiO_2+CNTs), on the other hand, due to nanotubes carbon have a high proportion and strong van der Waals forces, which make them well-dispersed and evenly distributed in the fluid. Viscosity range because MP-STF (SiO_2) tends to produce STFs with a narrow viscosity range, while DP-STF (SiO_2+CNTs) are capable of producing fluids with a broad range of viscosities [38]. This broad range is due to the self-assembly of CNTs, resulting in a network of entangled nanotubes that provide unique rheological properties. Shear stress sensitivity because MP-STF (SiO_2) is often more sensitive to changes in shear stress and can experience a sudden drop in viscosity at high shear rates [39]. DP-STF (SiO_2+CNTs), on the other hand, exhibit a higher tolerance to shear stress and can maintain their viscosity at high shear rates. Applications because DP-STF (SiO_2+CNTs) was applied in a wider range of fields, including aerospace, defense, biomedical, and electronics industries, thanks to their unique properties. MP-STF (SiO_2), however, are more limited in their applications due to their less desirable properties [40]. Finally, DP-STF (SiO_2+CNTs) are superior to MP-STF (SiO_2) due to their superior dispersion, broader viscosity range, higher tolerance to shear stress, and a wider range of applications.

Dual-phase suspensions are a type of composite material that offer unique properties and advantages compared to traditional monophase materials [41]. In this case, the dual-phase material is composed of a combination of CNT + SiO_2/ρ-Aramid, M-MWNT + SiO_2/ρ-Aramid, GO + SiO_2/ρ-Aramid, Gr + SiO_2/ρ-Aramid, which is made up of carbon nanotubes (CNTs), multi-wall carbon nanotubes (M-MWNT), graphene oxide (GO), graphene (Gr), silica dioxide (SiO_2) and ρ-Aramid fabrics. Their exceptional the 2° phase dispersed (CNTs, GO, Gr, and M-MWNT) promotes strength, stiffness, and thermal conductivity making it a material with great potential in the design of advanced STF for several applications in engineering and smart material technologies. Dual-phase STFs are dilatant fluids that combine a second phase and disperse the first phase (SiO_2). The second phase can be used nanoparticles of one, two, or three dimensions (1-D, 2-D, or 3-D) that enhance the rheological and application properties, thus the dual-phase STF are more versatile and have great value and high engineering properties. For example, it can be used in the production of the lightweight, high-force of yarn pull-out, as well protective gear manufacturing for military and police, as well as, in the production of sports equipment such as helmets and body armor-based innovative materials impregnated with STF. Dual-phase shear thickening fluids are a

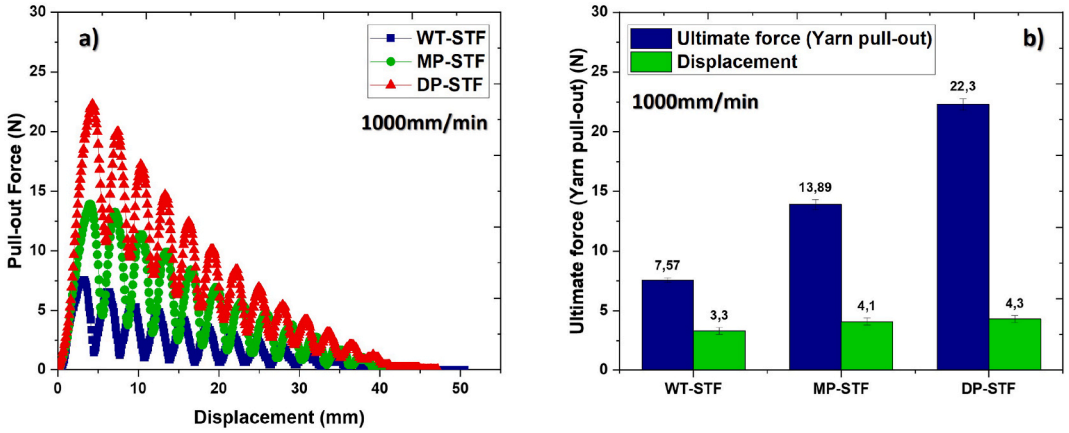

Fig. 9. Results of force versus displacement of the WT-STF, MP-STF, and DP-STF.

Table 4
Results ANOVA in WT-STF, MP-STF, and, DP-STF.

	Yarn pull-out force		Shear stress (Kinetic)		Shear stress (Static)		Friction energy	
	F value	***ρ-value***	***F value***	***ρ-value***	***F value***	***ρ-value***	***F value***	***ρ-value***
Model	4499.9	<0.0001	4592.8	<0.0001	4631.5	<0.0001	1132038.2	<0.0001
A - Composition	10750.2	<0.0001	11474.2	<0.0001	12113.0	<0.0001	2729297.3	<0.0001
B - Pull-out speed	1459.8	<0.0001	1136.1	<0.0001	961.0	<0.0001	334397.7	<0.0001
AB	1289.7	<0.0001	1168.0	<0.0001	820.7	<0.0001	332419.6	<0.0001
STD	0.262		0.425		0.425		0.467	
Mean	10.6		17.13		18.3		283.0	
C.V. %	2.46		2.48		2.32		0.17	
R^2	0.99		0.99		0.99		0.99	

promising technology that has unique properties that can be tailored to meet specific needs. Its potential applications are numerous and diverse, making it an exciting area of research in the field of material science. These combinations of CNT + SiO_2/ρ-Aramid [42, 43], M-MWNT + SiO_2/ρ-Aramid [24], GO + SiO_2/ρ-Aramid [43], Gr + SiO_2/ρ-Aramid [42,44], promote high loads, lightweight, the

Table 5
Top 10 articles applied to a yarn pull-out test.

					Friction between yarns		
Author	Journal	Year	Reference	STF/fabric base	Test speed	Ultimate Force	Displacement
Santos, Thiago et al.	–	2023	This paper	CNT + SiO2/ ρ-Aramid	1000 mm/ min	21.9 N	11.3 mm
Katiyar, Ajay et al.	Journal of Polymer Research	2021	[42]	Gr + SiO_2/ρ-Aramid	300 mm/ min	41 N	3 mm
				CNT + SiO_2/ ρ-Aramid		33 N	6.4 mm
Zhang, Junshuo et al.	Composites Part A	2021	[46]	SiO2/ρ-Aramid	600 mm/ min	11.6 N	2.4 mm
Santos, Thiago F. et al.	Journal of Composite Materials	2020	[14]	SiO2/ρ-Aramid	100 mm/ min	10.50 N	4 mm
Liu, Lulu et al.	Thin-Walled Structures	2020	[43]	CNT + SiO_2/ ρ-Aramid	50 mm/ min	10.0 N	–
				GO + SiO_2/ρ-Aramid	500 mm/ min	11.3 N	
Bai, Ruixiang et al.	Composites Part B	2019	[47]	SiO2/ρ-Aramid	1000 mm/ min	74.20 N	**18.4 mm**
Yeh, Shu-Kai et al.	Journal of Polymer Research	2019	[48]	SiO2/ρ-Aramid	80 mm/ min	35.3 N	4.2 mm
Feng, Yang et al.	IOP Conference Series: Materials Science and Engineering	2018	[49]	SiO2/ρ-Aramid	100 mm/ min	68.1 N	19.6 mm
Tan, Zhuhua et al.	Smart Materials and Structures	2018	[44]	Gr + SiO2/ρ-Aramid	400 mm/ min	29.8 N	6.4 mm
Li, Danyang et al.	Polymers	2018	[24]	M-MWNT + SiO2/ ρ-Aramid	100 mm/ min	30 N	4.8 mm

static and kinetic friction interfaces and the energy absorbed by the interface between the yarn and the STF make it an excellent choice for component applied to personal protection that needs to withstand and stresses. The CNT + SiO_2/ρ-Aramid, M-MWNT + SiO_2/-ρ-Aramid, GO + SiO_2/ρ-Aramid, Gr + SiO_2/ρ-Aramid dual-phase material has numerous potential applications, and offers a unique combination of properties that make it an attractive option for several applications in engineering and smart material technologies like sports products, medical products, space technology, and protection, and shielding products [45] exhibited Table 5.

5. Conclusions

Shear thickening fluids belong to the category of non-Newtonian fluids that shows a pronounced upsurge in viscosity when subjected to applied shear stress. These fluids demonstrate a nonlinear escalation in viscosity with higher shear rates or applied stress levels. Dual-phase of CNT-SiO_2 (DP-STF) in shear thickening fluids has been shown to significantly improve their performance compared to STFs with SiO_2 (MP-STF). The presence of CNTs creates a more interconnected network structure within the fluid, which enhances its ability to resist deformation and shear thickening behavior. However, MP-STF does not exhibit the same level of improvement in the fluid's properties. Although it can still contribute to the formation of a network structure, it lacks the specific properties that allow for efficient interparticle interaction and reinforcement, which are necessary for optimal STFs behavior. The results suggest that the DP-STF can significantly enhance their properties (force of yarn pull-out, the energy consumed by the interface, static and kinetic friction interface) and potential applications, particularly in areas such as protective clothing, sports equipment, and automotive engineering, where such shear thickening fluids can provide improved impact resistance and energy absorption. The nanoparticles, SiO_2+CNTs (DP-STF), significantly improved the properties of STFs, including their static and kinetic interfacial friction. This is because CNTs have a high aspect ratio, which allows them to form a network-like structure within the STF. CNTs have high surface energy and bond strongly with the STF, further enhancing the frictional properties. In contrast, SiO_2 nanoparticles alone do not have the same aspect ratio or surface energy as CNTs and may not be able to form a strong network within the STF. As a result, the static interfacial friction of SiO_2-based STFs (MP-STF) may be inferior to those using SiO2+CNTs (DP-STF). DP-STF have wide applicability in industrial and engineering uses, such as in shock absorbers and body armor, protective clothing, as well sports equipment, due to their ability to provide enhanced impact resistance and energy absorption.

Ethical approval

Not Applicable.

Funding

Not Applicable.

Author contribution statement

Thiago F. Santos, Caroliny M. Santos, Sanjay Mavinkere Rangappa, Suchart Siengchin, J. H. O. Nascimento: Conceived and designed the experiments; Performed the experiments; Analyzed and interpreted the data; Contributed reagents, materials, analysis tools or data; Wrote the paper.

Data availability statement

Data included in article/supp. material/referenced in article.

Declaration of competing interest

The authors declare that they have no known competing financial interests or personal relationships that could have appeared to influence the work reported in this paper.

Acknowledgements

The authors acknowledge the CARREFOUR group and the Graduate Program in Chemical Engineering at the Federal University of Rio Grande do Norte (PPGEQ/UFRN), for the financial and technical support.

References

[1] M.M. Moure, N. Feito, J. Aranda-Ruiz, J.A. Loya, M. Rodriguez-Millan, On the characterization and modeling of high-performance para-aramid fabrics, Compos. Struct. 212 (2019) 326–337, https://doi.org/10.1016/j.compstruct.2019.01.049.

[2] Y. Chu, S. Min, X. Chen, Numerical study of inter-yarn friction on the failure of fabrics upon ballistic impacts, Mater. Des. 115 (2017) 299–316, https://doi.org/10.1016/j.matdes.2016.11.013.

[3] Y. Chu, M.R. Rahman, S. Min, X. Chen, Experimental and numerical study of inter-yarn friction affecting mechanism on the ballistic performance of Twaron® fabric, Mech. Mater. 148 (2020), 103421, https://doi.org/10.1016/j.mechmat.2020.103421.

[4] R. Bai, W. Li, Z. Lei, Y. Ma, F. Qin, Q. Fang, X. Chen, Y. Chen, Experimental study of yarn friction slip and fabric shear deformation in yarn pull-out test, Compos. Part A Appl. Sci. Manuf. 107 (2018) 529–535, https://doi.org/10.1016/j.compositesa.2018.02.001.

[5] T. Santos, C. Santos, M. Aquino, S. Mavinkere Rangappa, S. Siengchin, J.H.O. Nascimento, I. Medeiros, Effects of UV sensitivity and accelerated photo-aging on stab resistance of ρ-aramid fabrics impregnated with shear thickening fluids (STFs), Heliyon 9 (2023), e15020, https://doi.org/10.1016/J.HELIYON.2023.E15020.

[6] R. Żurowski, M. Tryznowski, S. Gürgen, M. Szafran, A. Świderska, The influence of UV radiation aging on degradation of shear thickening fluids, Materials 15 (2022) 3269, https://doi.org/10.3390/ma15093269.

[7] A.F. Ávila, A.M. de Oliveira, S.G. Leão, M.G. Martins, Aramid fabric/nano-size dual phase shear thickening fluid composites response to ballistic impact, Compos. Part A Appl. Sci. Manuf. 112 (2018) 468–474, https://doi.org/10.1016/j.compositesa.2018.07.006.

[8] S. Gürgen, M.A. Sofuoğlu, M.C. Kuşhan, Rheological compatibility of multi-phase shear thickening fluid with a phenomenological model, Smart Mater. Struct. 28 (2019), 35027, https://doi.org/10.1088/1361-665X/ab018c.

[9] S. Gürgen, M.A. Sofuoğlu, M.C. Kuşhan, Rheological modeling of multi-phase shear thickening fluid using an intelligent methodology, J. Brazilian Soc. Mech. Sci. Eng. 42 (2020) 605, https://doi.org/10.1007/s40430-020-02681-z.

[10] S. Gürgen, M.C. Kuşhan, The ballistic performance of aramid based fabrics impregnated with multi-phase shear thickening fluids, Polym. Test. 64 (2017) 296–306, https://doi.org/10.1016/j.polymertesting.2017.11.003.

[11] M.R. Sheikhi, S. Gürgen, Anti-impact design of multi-layer composites enhanced by shear thickening fluid, Compos. Struct. 279 (2022), 114797, https://doi.org/10.1016/j.compstruct.2021.114797.

[12] F. Wang, C. An, Q. Jia, Effect of multi-phase STF on the high-speed impact performance of shear-thickening fluid (STF)-impregnated Kevlar Composite Fabrics, J. Phys. Conf. Ser. 1759 (2021), 012015, https://doi.org/10.1088/1742-6596/1759/1/012015.

[13] M.P. Ribeiro, P.H.P.M. da Silveira, F. de Oliveira Braga, S.N. Monteiro, Fabric impregnation with shear thickening fluid for ballistic armor polymer composites: an updated overview, Polymers 14 (2022) 4357, https://doi.org/10.3390/polym14204357.

[14] T.F. Santos, C.M. Santos, R.T. Fonseca, K.M. Melo, M.S. Aquino, F.R. Oliveira, J.I. Medeiros, Experimental analysis of the impact protection properties for Kevlar® fabrics under different orientation layers and non-Newtonian fluid compositions, J. Compos. Mater. (2020), https://doi.org/10.1177/0021998320916231.

[15] A. Khodadadi, G. Liaghat, A. Sabet, H. Hadavinia, A. Aboutorabi, O. Razmkhah, M. Akbari, M. Tahmasebi, Experimental and Numerical Analysis of Penetration into Kevlar Fabric Impregnated with Shear Thickening Fluid, 2017, https://doi.org/10.1177/0892705717704485.

[16] X. Zhang, R. Yan, Q. Zhang, L. Jia, The numerical simulation of the mechanical failure behavior of shear thickening fluid/fiber composites: a review, Polym. Adv. Technol. 33 (2022) 20–33, https://doi.org/10.1002/pat.5512.

[17] S. Gürgen, Numerical modeling of fabrics treated with multi-phase shear thickening fluids under high velocity impacts, Thin-Walled Struct. 148 (2020), 106573, https://doi.org/10.1016/j.tws.2019.106573.

[18] A. Majumdar, B.S. Butola, A. Srivastava, B. Singh Butola, A. Srivastava, Optimal designing of soft body armour materials using shear thickening fluid, Mater. Des. 46 (2013) 191–198, https://doi.org/10.1016/j.matdes.2012.10.018.

[19] T.F. Santos, C.M. Santos, M.S. Aquino, F.R. Oliveira, J.I. Medeiros, Statistical study of performance properties to impact of Kevlar® woven impregnated with Non-Newtonian Fluid (NNF), J. Mater. Res. Technol. 9 (2020) 3330–3339, https://doi.org/10.1016/j.jmrt.2020.01.027.

[20] L. Zílio, M. Dias, T. Santos, C. Santos, R. Fonseca, A. Amaral, M. Aquino, Characterization and statistical analysis of the mechanical behavior of knitted structures used to reinforce composites: yarn compositions and float stitches, J. Mater. Res. Technol. 9 (2020) 8323–8336, https://doi.org/10.1016/j.jmrt.2020.05.089.

[21] T.F. dos Santos, C.M. da S. Santos, D. Ionesi, M.S. de Aquino, I. Medeiros, Influence of silane coupling agent on shear thickening fluids (STF) for personal protection, J. Mater. Res. Technol. (2019), https://doi.org/10.1016/j.jmrt.2019.07.013.

[22] T.F. Santos, C.M. Santos, M. Dias, L. Zilio, K.M. Melo, M.E. Cavalcante, L.F. Castro, E.K. Hussein, M.S. Aquino, Mechanical behavior of natural/synthetic weft-knitted structures commonly used as reinforcement of hybrid composites via full factorial design: yarn compositions and float stitches, in: Green Hybrid Compos. Eng. Non-engineering Appl., 2023, https://doi.org/10.1007/978-981-99-1583-5_15.

[23] L. Zílio, M. Dias, T. Santos, C. Santos, R. Fonseca, A. Amaral, M. Aquino, Characterization and statistical analysis of the mechanical behavior of knitted structures used to reinforce composites: yarn compositions and float stitches, J. Mater. Res. Technol. 9 (2020) 8323–8336, https://doi.org/10.1016/j.jmrt.2020.05.089.

[24] D. Li, R. Wang, X. Liu, S. Fang, Y. Sun, Shear-thickening fluid using oxygen-plasma-modified multi-walled carbon nanotubes to improve the quasi-static stab resistance of kevlar fabrics, Polymers 10 (2018) 1356, https://doi.org/10.3390/polym10121356.

[25] S. Gürgen, M.C. Kuşhan, W. Li, Shear thickening fluids in protective applications: a review, Prog. Polym. Sci. 75 (2017) 48–72, https://doi.org/10.1016/j.progpolymsci.2017.07.003.

[26] S. Gürgen, M.C. Kuşhan, The stab resistance of fabrics impregnated with shear thickening fluids including various particle size of additives, Compos. Part A Appl. Sci. Manuf. 94 (2017) 50–60, https://doi.org/10.1016/j.compositesa.2016.12.019.

[27] M. Bajya, A. Majumdar, B.S. Butola, Criticality of inter-yarn friction in high-performance fabrics for the design of soft body armour, Compos. Commun. 29 (2022), 100984, https://doi.org/10.1016/j.coco.2021.100984.

[28] C.M. Schneider, H. Cölfen, Formation of nanoclusters in gold nucleation, Crystals 10 (2020) 382, https://doi.org/10.3390/cryst10050382.

[29] J. Zhang, Y. Wang, J. Zhou, J. Wu, S. Liu, M. Sang, B. Liu, Y. Pan, X. Gong, Multi-functional STF-based yarn for human protection and wearable systems, Chem. Eng. J. 453 (2023), 139869, https://doi.org/10.1016/j.cej.2022.139869.

[30] M.A. Abtew, F. Boussu, P. Bruniaux, Dynamic impact protective body armour: a comprehensive appraisal on panel engineering design and its prospective materials, Def. Technol. 17 (2021) 2027–2049, https://doi.org/10.1016/j.dt.2021.03.016.

[31] Y. Zhou, M. Ali, X. Gong, D. Yang, An overview of yarn pull-out behavior of woven fabrics, Textil. Res. J. 89 (2019) 223–234, https://doi.org/10.1177/0040517517741156.

[32] M. Wei, K. Lin, L. Sun, Shear thickening fluids and their applications, Mater. Des. 216 (2022), 110570, https://doi.org/10.1016/j.matdes.2022.110570.

[33] S. Alikarami, N. Kordani, A. SadoughVanini, H. Amiri, Effect of the yarn pull-out velocity of shear thickening fluid-impregnated Kevlar fabric on the coefficient of friction, J. Mech. Sci. Technol. 30 (2016) 3559–3565, https://doi.org/10.1007/s12206-016-0716-2.

[34] Z. Xie, W. Chen, Y. Liu, L. Liu, Z. Zhao, G. Luo, Design of the ballistic performance of shear thickening fluid (STF) impregnated Kevlar fabric via numerical simulation, Mater. Des. 226 (2023), 111599, https://doi.org/10.1016/j.matdes.2023.111599.

[35] U. Mawkhlieng, A. Majumdar, A. Laha, A review of fibrous materials for soft body armour applications, RSC Adv. 10 (2020) 1066–1086, https://doi.org/10.1039/C9RA06447H.

[36] E.D. LaBarre, X. Calderon-Colon, M. Morris, J. Tiffany, E. Wetzel, A. Merkle, M. Trexler, Effect of a carbon nanotube coating on friction and impact performance of Kevlar, J. Mater. Sci. 50 (2015) 5431–5442, https://doi.org/10.1007/s10853-015-9088-8.

[37] K.M. De Melo, T.F. Dos Santos, C.M.D.S. Santos, R.T. Da Fonseca, N.D. De Lucena, J.I. De Medeiros, M.S. De Aquino, Study of the reuse potential of the sisal fibers powder as a particulate material in polymer composites, J. Mater. Res. Technol. 8 (2019) 4019–4025, https://doi.org/10.1016/j.jmrt.2019.07.010.

[38] Y. Tan, Y. Ma, Y. Li, Shear thickening fabric composites for impact protection: a review, Textil. Res. J. 93 (2023) 1419–1444, https://doi.org/10.1177/00405175221126746.

[39] R. Kotsilkova, S. Tabakova, Exploring effects of graphene and carbon nanotubes on rheology and flow instability for designing printable polymer nanocomposites, Nanomaterials 13 (2023) 835, https://doi.org/10.3390/nano13050835.

[40] V. Pais, P. Silva, J. Bessa, H. Dias, M.H. Duarte, F. Cunha, R. Fangueiro, Low-velocity impact response of auxetic seamless knits combined with non-Newtonian fluids, Polymers 14 (2022) 2065, https://doi.org/10.3390/polym14102065.

[41] M.R. Sheikhi, M. Hasanzadeh, Multi-phase shear thickening fluid, in: Shear Thick. Fluid, Springer International Publishing, Cham, 2023, pp. 33–51, https://doi.org/10.1007/978-3-031-25717-9_3.

[42] A. Katiyar, T. Nandi, P. Katiyar, Energy absorption of graphene and CNT infused hybrid shear thickening fluid embedded textile fabrics, J. Polym. Res. 28 (2021) 334, https://doi.org/10.1007/s10965-021-02697-6.
[43] L. Liu, M. Cai, X. Liu, Z. Zhao, W. Chen, Ballistic impact performance of multi-phase STF-impregnated Kevlar fabrics in aero-engine containment, Thin-Walled Struct. 157 (2020), 107103, https://doi.org/10.1016/j.tws.2020.107103.
[44] Z. Tan, W. Li, W. Huang, The effect of graphene on the yarn pull-out force and ballistic performance of Kevlar fabrics impregnated with shear thickening fluids, Smart Mater. Struct. 27 (2018), 075048, https://doi.org/10.1088/1361-665X/aaca4b.
[45] M. Zarei, J. Aalaie, Application of shear thickening fluids in material development, J. Mater. Res. Technol. 9 (2020) 10411–10433, https://doi.org/10.1016/j.jmrt.2020.07.049.
[46] J. Zhang, Y. Wang, J. Zhou, C. Zhao, Y. Wu, S. Liu, X. Gong, Intralayer interfacial sliding effect on the anti-impact performance of STF/Kevlar composite fabric, Compos. Part A Appl. Sci. Manuf. 145 (2021), 106401, https://doi.org/10.1016/j.compositesa.2021.106401.
[47] R. Bai, Y. Ma, Z. Lei, Y. Feng, C. Liu, Energy analysis of fabric impregnated by shear thickening fluid in yarn pullout test, Compos. B Eng. 174 (2019), 106901, https://doi.org/10.1016/j.compositesb.2019.106901.
[48] S.-K. Yeh, J.-J. Lin, H.-Y. Zhuang, Y.-C. Chen, H.-C. Chang, J.-Y. Zheng, L.-Y. Yang, K.-C. Lee, Y.-L. Chen, S.-P. Rwei, Light shear thickening fluid (STF)/Kevlar composites with improved ballistic impact strength, J. Polym. Res. 26 (2019) 155, https://doi.org/10.1007/s10965-019-1811-8.
[49] Y. Feng, Y. Ma, Z. Lei, S. Cao, Q. Fang, W. Li, R. Bai, S. Xuan, Experimental study on yarn pullout test of STF modified fabric, IOP Conf. Ser. Mater. Sci. Eng. 381 (2018), 012111, https://doi.org/10.1088/1757-899X/381/1/012111.